Available online at www.sciencedirect.com
SCIENCE DIRECT®
Journal of Solid State Chemistry 178 (2005) 3169–3175
JOURNAL OF SOLID STATE CHEMISTRY
www.elsevier.com/locate/jssc

Synthesis, structure, and electronic structure of K_2CuSbS_3

Bin Deng[a], George H. Chan[a], Donald E. Ellis[a,b], Richard P. Van Duyne[a], James A. Ibers[a,*]

[a]*Department of Chemistry, Northwestern University, 2145 Sheridan Road, Evanston, IL 60208-3113, USA*
[b]*Department of Physics and Astronomy, Northwestern University, 2145 Sheridan Road., Evanston, IL 60208-3113, USA*

Received 13 June 2005; received in revised form 21 July 2005; accepted 26 July 2005
Available online 31 August 2005

Abstract

The new compound K_2CuSbS_3 has been synthesized by the reaction of K_2S, Cu, Sb, and S at 823 K. The compound crystallizes in the Na_2CuSbS_3 structure type with four formula units in space group $P2_1/c$ of the monoclinic system in a cell at 153 K of $a = 6.2712$ (6) Å, $b = 17.947$ (2) Å, $c = 7.4901$ (8) Å, $\beta = 120.573$ (1)°, and $V = 725.81$ (12) Å^3. The structure contains two-dimensional $^2_\infty$[$CuSbS_3$] layers separated by K atoms. Each $^2_\infty$[$CuSbS_3$] layer is built from CuS_3 and SbS_3 units. Each Cu atom is pyramidally coordinated to three S atoms with the Cu atom about 0.4 Å above the plane of the S atoms. Each Sb atom is similarly coordinated to three S atoms but is about 1.1 Å above its S_3 plane. First-principles calculations indicate an indirect band gap of 1.9 eV. These calculations also indicate that there is a bonding interaction between the Cu and Sb atoms. An optical absorption measurement performed with light perpendicular to the (0 1 0) crystal face of a red block-shaped crystal of K_2CuSbS_3 indicates an experimental indirect band gap of 2.2 eV.
© 2005 Elsevier Inc. All rights reserved.

Keywords: Dipotassium copper antimony trisulfide; Crystal structure; Electronic structure; Band gap

1. Introduction

The thioantimonates of the coinage metals, both the M/Sb/S ternaries and the A/M/Sb/S quaternaries, where M = Cu, Ag, or Au and A = alkali metal, display considerable structural and compositional complexity. In the series, Sb can have a formal oxidation state of 3+ or 5+ or both. For example, the formal oxidation state of Sb is 3+ in Na_2CuSbS_3 [1], 5+ in A_2AgSbS_4 (A = K, Rb, Cs) [2,3], and 3+, 3+, and 5+ in $Cs_3Ag_2Sb_3S_8$ [3]. The stereochemically active $5s^2$ lone-pair electrons influence the structures that contain Sb^{3+}. In particular, the Cu–Sb distance in γ-Cu_3SbS_3 of 2.61 (1) Å [4] is comparable to that of 2.627 (1) Å in Cu_2Sb [5].

In order to understand the Cu–Sb interaction in compounds where the formal oxidation states are Cu^{1+} and Sb^{3+}, the new compound, K_2CuSbS_3 was synthesized by the reactive flux method [6]. Here we report its crystal structure and optical properties, and a first principles calculation of its electronic structure.

2. Experimental section

2.1. Synthesis

The following reagents were used as received: K (Aldrich, 99.9%), Cu (Aldrich, 99.99%), Sb (Aldrich, 99.5%), and S (Alfa Aesar, 99.5%). K_2S was prepared by the stoichiometric reaction of the elements in liquid ammonia. The compound K_2CuSbS_3 was synthesized by the addition of 1.0 mmol K_2S, 1.0 mmol Sb, 1.0 mmol Cu, and 2.0 mmol S into a fused-silica tube under an argon atmosphere in a glove box. The tube was sealed under a 10^{-4} Torr atmosphere and then placed in a computer-controlled furnace. The sample was heated to 823 K in 10 h, kept at 823 K for 72 h, cooled at 4 K/h to 373 K, and then the furnace was turned off. The reaction product was washed with dimethylformamide and then

*Corresponding author. Fax: +1 847 491 2976.
E-mail address: ibers@chem.northwestern.edu (J.A. Ibers).

0022-4596/$ - see front matter © 2005 Elsevier Inc. All rights reserved.
doi:10.1016/j.jssc.2005.07.027

kept in a vacuum desiccator. The product consisted of red block-shaped crystals. The yield was approximately 50%. The side products, as determined by EDX analyses, were ternary K/Sb/S needles and binary Cu/S black blocks. The heating profile could not be adjusted to eliminate these side products, but it did affect the composition of these side products. Thus, when the reaction temperature was below 673 K the ternary K/Sb/S needles predominated; when the reaction temperature was above 973 K the binary Cu/S black blocks predominated. Examination of selected crystals with an EDX-equipped Hitachi S-3500 SEM indicated the presence of K, Cu, Sb, and S. The compound is not very stable in air; the red crystals exposed to air become black in about 1 h.

2.2. Structure determination

Single crystal X-ray diffraction data were obtained with the use of graphite-monochromatized Mo$K\alpha$ radiation ($\lambda = 0.71073$ Å) at 153 K on a Bruker Smart-1000 CCD diffractometer [7]. The crystal-to-detector distance was 5.023 cm. Crystal decay was monitored by recollecting 50 initial frames at the end of the data collection. Data were collected by a scan of 0.3° in ω in groups of 606 frames for each of the ϕ settings 0°, 120°, and 240°. The exposure time was 15 s/frame. Intensity data were collected with the program SMART [7]. Cell refinement and data reduction were carried out with the use of the program SAINT [7], and numerical face-indexed absorption corrections were performed with the use of the program XPREP [8]. Then the program SADABS [7] was employed to make incident beam and decay corrections.

The structure was solved with the direct-methods program SHELXS and refined with the full-matrix least-squares program SHELXL [8]. The final refinement included anisotropic displacement parameters and a secondary extinction correction. The program TIDY [9] was then employed to standardize the atomic coordinates. Additional experimental details are shown in Table 1 and in Supplementary information. Table 2 presents selected metrical data.

2.3. Electronic structure calculations

Electronic structure calculations of K_2CuSbS_3 and Cu_2Sb [5] were performed with the self-consistent, scalar relativistic linearized muffin-tin orbital program of Andersen and co-workers [10–12] within the atomic sphere approximation. In the calculations presented here, the von Barth–Hedin exchange-correlation potential was used within the local density approximation [13]. Interstitial spheres were introduced to achieve space filling. The radii (in atomic units, Bohr) were automatically determined to be 4.1 for K, 2.4 for Cu, 2.8 for Sb, and 2.5 for S in K_2CuSbS_3 and 2.6 for Cu and 3.3 for Sb in Cu_2Sb. The maximum overlap between any two atom centered spheres was not allowed to exceed 16%. The basis sets consisted of the valence 4*s* electrons for K, the 3*d* and 4*s* electrons for Cu, the 5*s* and 5*p* electrons for Sb, the 3*s* and 3*p* electrons for S, and 1*s* electrons for empty spheres. The 4*p* and 4*d* electrons for K, 5*d* electrons for Sb, and 3*d* electrons for S, and the *p*–*d* states for empty spheres were downfolded by means of the Löwdin technique [14]. The crystal orbital Hamiltonian population (COHP) [15], which is the density of states weighted by the corresponding Hamiltonian matrix element, was used to analyze the strength and nature of the bonds. Interatomic interactions were analyzed by integrating the area of the COHP curves up to the Fermi level. The ICOHP (Integrated COHP) values reflect qualitatively the strength of the bonds. All *k*-space integrations were performed with the tetrahedron method [16,17]. For K_2CuSbS_3 and Cu_2Sb 172 points and 142 *k* points were used in the Brillouin zone, respectively.

Table 1
Crystal data and structure refinement for K_2CuSbS_3

Formula mass	359.67
Space group	$P2_1/c$
a (Å)	6.2712 (6)
b (Å)	17.947 (2)
c (Å)	7.4901 (8)
β (deg)	120.573 (1)
V (Å^3)	725.81 (12)
Z	4
T (K)	153 (2)
λ (Å)	0.71073
ρ_c (g/cm^3)	3.291
μ (cm^{-1})	85.4
R (F)[a]	0.0223
R_w (F_o^2)[b]	0.0534

[a] $R(F) = \sum ||F_o| - |F_c|| / |F_o|$ for $F_o^2 > 2\sigma(F_o^2)$.
[b] $R_w(F_o^2) = \{\sum[w(F_o^2 - F_c^2)^2] / \sum wF_o^4\}^{1/2}$ for all data. $w^{-1} = \sigma^2(F_o^2) + (0.026F_o^2)^2$ for $F_o^2 \geq 0$ and $w^{-1} = \sigma^2(F_o^2)$ for $F_o^2 < 0$.

Table 2
Selected bond distances (Å) and bond angles (deg) for K_2CuSbS_3

K1–S3	3.0909(9)	K2–S3	3.193(1)
K1–S1	3.141(1)	K2–S1	3.195(1)
K1–S3	3.1836(9)	Cu–S3	2.2806(8)
K1–S2	3.278(1)	Cu–S2	2.2886(8)
K1–S2	3.358(1)	Cu–S2	2.3872(8)
K1–S1	3.440(1)	Sb–S1	2.3894(8)
K2–S3	3.129(1)	Sb–S3	2.4250(8)
K2–S2	3.140(1)	Sb–S2	2.4840(7)
K2–S1	3.161(1)	Cu–Sb	2.8554(5)
K2–S1	3.163(1)	S1–Sb–S3	99.22(3)
S3–Cu–S2	108.42(3)	S3–Sb–S2	101.20(2)
S3–Cu–S2	121.52(3)	S1–Sb–S2	100.31(2)
S2–Cu–S2	119.48(3)		

2.4. Optical absorption measurement

A single crystal of K_2CuSbS_3 of dimensions 108, 54, and 78 μm in the [1 0 0], [0 1 0], and [0 0 1] directions, respectively, was selected. An absorption measurement with light from a tungsten–halogen lamp polarized perpendicular to the [1 0 0] direction and impinging on the (0 1 0) crystal face was performed with the use of an Ocean Optics model S2000 spectrometer over the range of 400 nm (3.10 eV) to 800 nm (1.55 eV) at 293 K as described previously [18]. Because the compound is not very stable in air, comparisons of the optical absorption edge for light parallel and perpendicular to the unique axis could not be obtained [19]. The scaled absorption value and the crystal thickness were used to calculate the absorption coefficient α, as described previously [18]. From the fundamental absorption band edge, the optical band gap energy, E_g, was obtained from the relation $(\alpha h\nu)^{1/2} \approx h\nu - E_g$, which is suitable for an indirect transition [20,21]. The baseline and the absorption band edge were fit by least-squares lines; the intersection of these lines provided the value of the band gap.

3. Results

3.1. Synthesis

The new compound K_2CuSbS_3 was synthesized from the elements by means of the reactive flux method [6] at 823 K in 50% yield. The product is air sensitive. Note that the isostructural compound Na_2CuSbS_3 [1] was synthesized by a totally different route, namely by the reaction of Na_2CO_3, Cu, Sb_2S_3, and S in supercritical ethylenediamine at 350 °C.

3.2. Crystal structure

The crystal structure of K_2CuSbS_3 is illustrated in Fig. 1. It comprises layers perpendicular to [0 1 0]. The two-dimensional layers are formed by corner sharing between SbS_3 units and CuS_3 units, as indicated in Fig. 2. The layers are separated by K^+ cations. Because there are no S–S bonds in the structure the formal oxidation states of K/Cu/Sb/S can be assigned as 1+/1+/3+/2−. A valence bond sum calculation [22,23] is consistent with this assignment (Table 3).

Fig. 3 shows the coordination environments of Cu and Sb. The Cu atom is coordinated to three S atoms in a flattened trigonal pyramid. The distances of the Cu and S atoms from the CuS_3 least-squares plane are +0.328, −0.120, −0.100, and −0.108 Å. The Sb atom is coordinated to three S atoms in a trigonal pyramidal arrangement, with distances from the SbS_3 least-squares plane being −0.845, 0.286, 0.276, and 0.283 Å. The lone pair of electrons on the Sb^{3+} center is presumably located at the fourth coordination site to complete a distorted tetrahedron. The two unique K atoms are each coordinated by six S atoms.

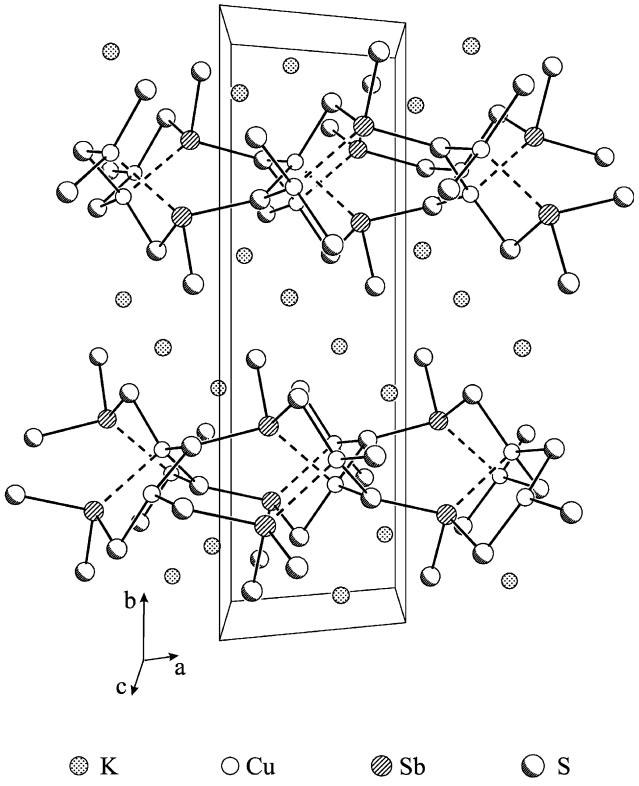

Fig. 1. The crystal structure of K_2CuSbS_3 viewed in the [0 0 1] direction.

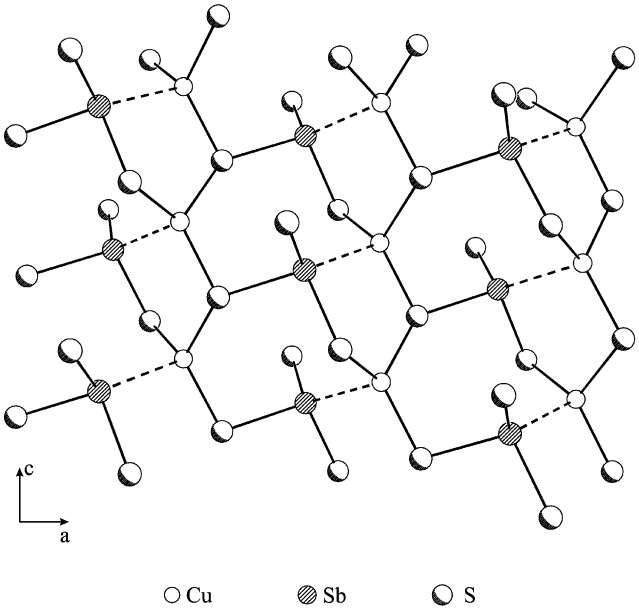

Fig. 2. The $^2_\infty[CuSbS_3]$ layer in K_2CuSbS_3 viewed down [0 1 0]. The Cu···Sb interaction is shown as a dashed line.

Table 3
Calculated bond valence sums for the atoms in K_2CuSbS_3

Atom	Bond valence sum	Formal charge
K1	0.98	+1
K2	1.09	+1
Cu	0.91	+1
Sb	2.83	+3
S1	1.82	−2
S2	1.96	−2
S3	2.02	−2

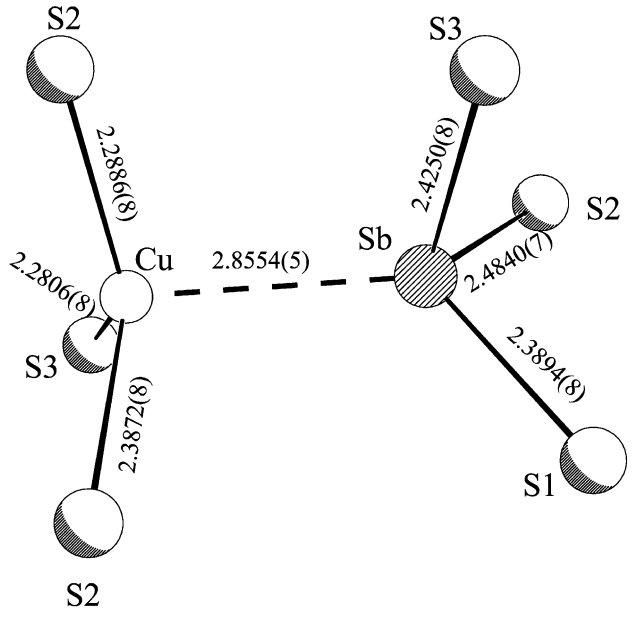

Fig. 3. The coordination environments of Cu and Sb in K_2CuSbS_3. Distances are in Å.

Selected metrical data for K_2CuSbS_3 are listed in Table 2. The K–S distances range from 3.0909(9) to 3.440(1) Å, comparable to those of 3.085(1) to 3.7198(8) Å in KY_2CuS_4 [24]. The Cu–S distances of 2.2806(8), 2.2886(8), and 2.3872(8) Å are in the range of those in Na_2CuSbS_3 (2.291(2), 2.279(2), and 2.345(2) Å) [1]. The Sb–S distances of 2.3894(8), 2.4250(8), and 2.4840(7) Å are also comparable to those of 2.389(2), 2.418(2), and 2.466(2) Å in Na_2CuSbS_3 [1]. The lone-pair electrons of Sb^{3+} are presumably located opposite to the plane of the three S atoms and point toward the Cu atom. The Cu–Sb distance is 2.8554(5) Å, which is comparable to that of 2.808(2) Å in Na_2CuSbS_3 [1]. Although shorter Cu–Sb distances are known, for example 2.627(1) Å in the alloy Cu_2Sb, 2.660(1) Å in $[C_2H_8N_2]_{0.5}[Cu_2SbS_3]$ [25], 2.706(9) Å in $[C_2N_2H_{10}]_{0.5}[Cu_2SbS_3]$ [26], 2.741(7) Å in $[C_3N_2H_{12}]_{0.5}[Cu_2SbS_3]$ [26], and 2.701(9) Å in $[C_4N_2H_{14}]_{0.5}[Cu_2SbS_3]$ [26], the distance found in the present compound is still indicative of a Cu···Sb interaction (see below).

3.3. Electronic structure and optical band gap

Fig. 4 shows the total density of states (DOS) and the contribution from the Cu, Sb, and S1 atoms. The K 4*s* states make minimal contributions around the Fermi level and thus are not included in the plots. The Cu 3*d*, Sb 5*p*, and S 3*p* states are highly hybridized in the region from −5 eV to the Fermi level, where Cu–S and Sb–S bonds are formed. The major peaks below −10 eV arise mainly from the S 3*s*, S 3*p*, Sb 5*s*, and Sb 5*p* states. The $5s^2$ lone-pair electrons of Sb are localized in the region from −9 to −8 eV. The Cu 3*d* states are located mainly in the valence band and make almost no contributions in the conduction band. The major states in the conduction band are a mixture of Sb and S states.

The band structure of K_2CuSbS_3 is shown in Fig. 5. The valence band maximum is located at the Γ (0, 0, 0) point, and the conduction band minimum is found at the A (−1/2, 1/2, 0) and B (−1/2, 0, 0) points. Therefore, the band gap is indirect, with a value of 1.9 eV. Fig. 6 shows the optical absorption spectrum of K_2CuSbS_3. A band gap of 2.2 eV was derived for an indirect transition. That the transition is indirect is consistent with the electronic structure calculations and with analysis of the diffuse reflectance spectrum of Na_2CuSbS_3, which led to an indirect band gap energy of 1.8 eV [1]. That the present electronic structure calculations underestimated the band gap energy of K_2CuSbS_3 probably can be attributed to the local density approximation [27]. Both the local density approximation and the generalized gradient approximation exchange-correlation potential improperly account for

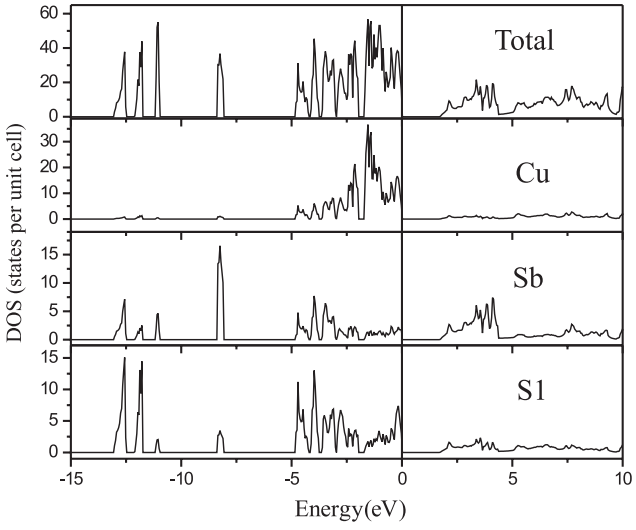

Fig. 4. The total and selected partial DOS of K_2CuSbS_3.

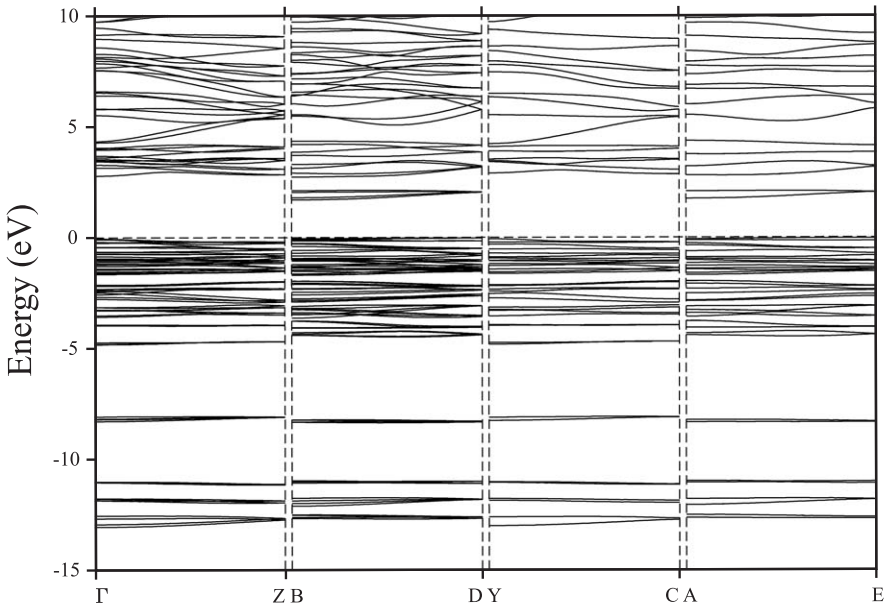

Fig. 5. The band structure of K_2CuSbS_3. The high symmetry points in the first Brillouin zone are Γ (0, 0, 0), Z (0, 0, ½) B (−1/2, 0, 0), D (−1/2, 0, 1/2), Y (0, 1/2, 0), C (0, 1/2, 1/2), A (−1/2, 1/2, 0), and E (−1/2, 1/2, 1/2).

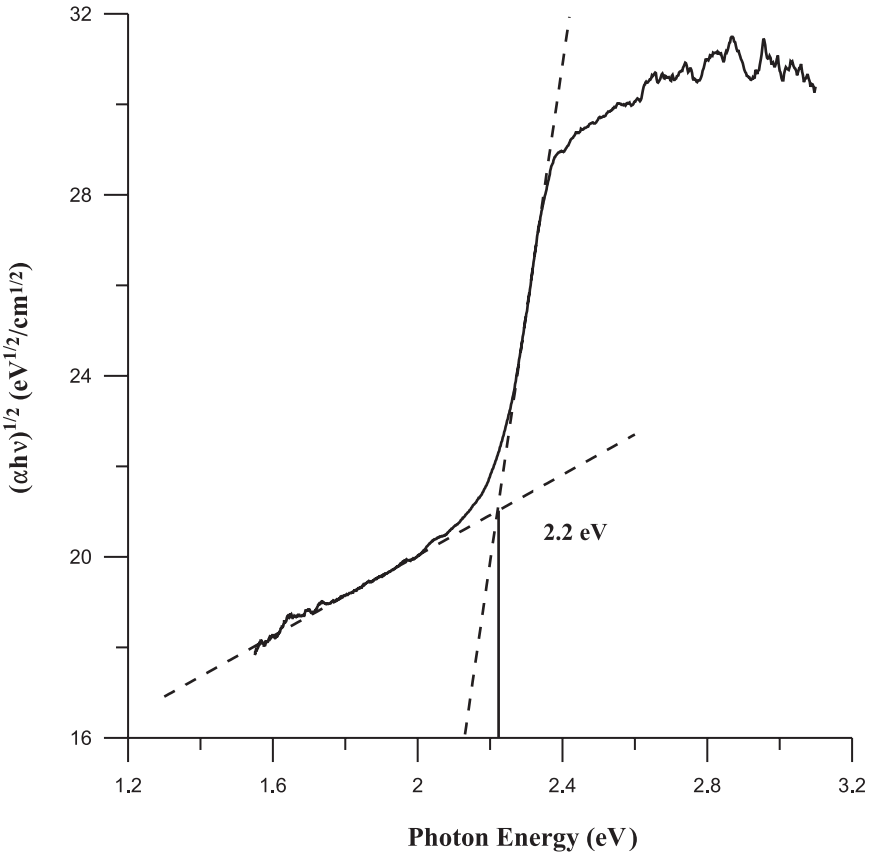

Fig. 6. Optical absorption spectrum of K_2CuSbS_3 obtained with light propagated in the [0 1 0] direction and polarized perpendicular to the [1 0 0] direction. The band gap has been derived for an indirect transition.

strongly correlated 3*d* electrons. However, the topology of the band structure is correctly provided by the local density approximation.

Fig. 7 presents crystal orbital Hamiltonian population (COHP) curves for the Cu···Sb interaction and for representative Cu–S and Sb–S bonds. The energy

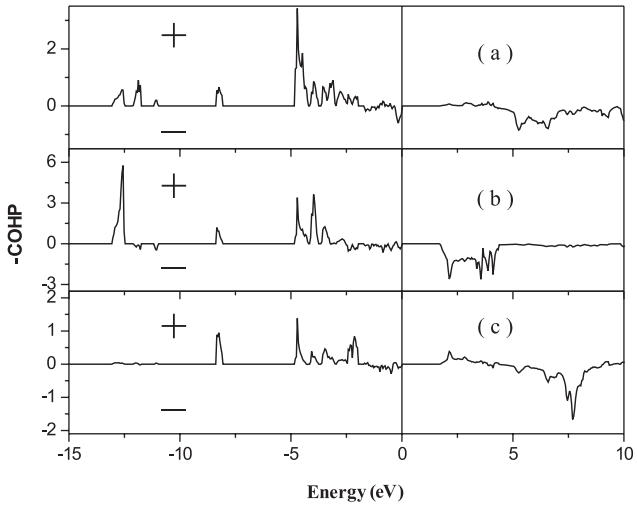

Fig. 7. –COHP curves for representative bonds in K_2CuSbS_3: (a) Cu–S2 (2.3872(8) Å); (b) Sb–S2 (2.4840(7) Å); (c) Cu···Sb (2.8554(5) Å). The + region is bonding and the − region is antibonding.

Table 4
ICOHP values for selected bonds in K_2CuSbS_3 and Cu_2Sb

Bond	Distance (Å)	ICOHP (eV/bond)
K_2CuSbS_3		
Sb–S2	2.4870(7)	−2.45
Cu–S2	2.3872(8)	−1.90
Cu–Sb	2.8554(5)	−0.78
Cu_2Sb		
Sb–Cu2	2.627(1)	−1.54
Sb–Cu1	2.701(1)	−1.18
Sb–Cu2	2.834(1)	−0.86

sequence of the three kinds of bond COHPs is Sb–S > Cu–S > Cu–Sb. As shown in Fig. 7, the Sb–S and Cu–S bonds are formed in three energy regions: −14 to −10 eV, −9 to −8 eV, and −5 eV to the Fermi level. The Cu···Sb bonding interaction only appears in the latter two regions. Note that the peak located around −8.5 eV arises mainly from $5s^2$ lone-pair electrons of Sb^{3+}. Therefore, the lone-pair electrons are also partially shared by Cu, which results in a bonding interaction between Cu and Sb. For comparison, we also calculated the COHP for the Cu–Sb bond in the alloy Cu_2Sb.

Table 4 lists the ICOHP values for selected bonds in K_2CuSbS_3 and Cu_2Sb. The bond strengths are Sb–S > Cu–S > Cu–Sb. The Cu–Sb (2.8554(5) Å) bond in K_2CuSbS_3 has an ICOHP value of −0.78 eV per bond, which is comparable to the Sb–Cu2 (2.834(1) Å) bond of −0.86 eV per bond in Cu_2Sb.

4. Supplementary material

Crystallographic data in cif format for K_2CuSbS_3 have been deposited as CSD number 415483. These data may be obtained free of charge by contacting FTZ Karlsruhe at +49 7247 808 666 (fax) or crysdata@fiz-karlsruhe.de (email).

Acknowledgments

This research was supported in part by National Science Foundation Grant DMR00-96676. Use was made of the Central Facilities supported by the MRSEC program of the National Science Foundation (DMR00-76097) at the Materials Research Center of Northwestern University.

Appendix A. Supplementary Material

The online version of this article contains additional supplementary data. Please visit doi:10.1016/j.jssc.2005.07.027.

References

[1] J.E. Jerome, G.L. Schimek, G.W. Drake, J.W. Kolis, Eur. J. Solid State Inorg. Chem. 33 (1996) 765–782.
[2] G.L. Schimek, W.T. Pennington, P.T. Wood, J.W. Kolis, J. Solid State Chem. 123 (1996) 277–284.
[3] P.T. Wood, G.L. Schimek, J.W. Kolis, Chem. Mater. 8 (1996) 721–726.
[4] A. Pfitzner, Z. Kristallogr. 213 (1998) 228–236.
[5] J. Nuss, M. Jansen, Z. Anorg. Allg. Chem. 628 (2002) 1152–1157.
[6] S.A. Sunshine, D. Kang, J.A. Ibers, J. Am. Chem. Soc. 109 (1987) 6202–6204.
[7] Bruker, SMART Version 5.054 Data Collection and SAINT-Plus Version 6.45a Data Processing Software for the SMART System, Bruker Analytical X-ray Instruments, Inc., Madison, WI, USA, 2003.
[8] G.M. Sheldrick, SHELXTL Version 6.14, Bruker Analytical X-ray Instruments, Inc., Madison, WI, USA, 2003.
[9] L.M. Gelato, E. Parthé, J. Appl. Crystallogr. 20 (1987) 139–143.
[10] O.K. Andersen, Phys. Rev. B 12 (1975) 3060–3083.
[11] O.K. Andersen, O. Jepsen, Phys. Rev. Lett. 53 (1984) 2571–2574.
[12] O. Jepsen, O.K. Andersen, Z. Phys. B: Condens. Matter 97 (1995) 35–47.
[13] L. Hedin, B.I. Lundqvist, J. Phys. Chem. Solids 4 (1971) 2064–2083.
[14] P.-O. Löwdin, J. Chem. Phys. 19 (1951) 1396–1401.
[15] R. Dronskowski, P.E. Blöchl, J. Phys. Chem. 97 (1993) 8617–8624.
[16] W.R.L. Lambrecht, O.K. Andersen, Phys. Rev. B 34 (1986) 2439–2449.

[17] O. Jepsen, O.K. Andersen, Solid State Commun. 9 (1971) 1763–1767.
[18] K. Mitchell, F.Q. Huang, E.N. Caspi, A.D. McFarland, C.L. Haynes, R.C. Somers, J.D. Jorgensen, R.P. Van Duyne, J.A. Ibers, Inorg. Chem. 43 (2004) 1082–1089.
[19] T. Matsumoto, M. Aoki, A. Kinoshita, T. Aono, Jpn. J. Appl. Phys. 13 (1974) 737–738.
[20] T.-H. Bang, S.-H. Choe, B.-N. Park, M.-S. Jin, W.-T. Kim, Semicond. Sci. Technol. 11 (1996) 1159–1162.
[21] J.I. Pankove, Optical Processes in Semiconductors, Prentice-Hall, Inc., Englewood Cliffs, NJ, 1971.
[22] I.D. Brown, Struct. Bonding Cryst. II (1981) 1–30.
[23] S. Adams, Acta Crystallogr. Sect. B: Struct. Sci. 57 (2001) 278–287.
[24] J. Yao, B. Deng, D.E. Ellis, J.A. Ibers, J. Solid State Chem. 176 (2003) 5–12.
[25] A.V. Powell, S. Boissière, A.M. Chippindale, J. Chem. Soc. Dalton Trans. (2000) 4192–4195.
[26] V. Spetzler, H. Rijnberk, C. Näther, W. Bensch, Z. Anorg. Allg. Chem. 630 (2004) 142–148.
[27] M.S. Hybertsen, S.G. Louie, Phys. Rev. B 34 (1986) 5390–5413.